CI&CEQ
Chemical Industry & Chemical Engineering Quarterly

Available online at
Association of the Chemical Engineers of Serbia AChE
www.ache.org.rs/CICEQ

Chem. Ind. Chem. Eng. Q. 29 (2) 87–98 (2023) CI&CEQ

RAJASEKAR SUBRAMANYAM
MEYYAPPAN NARAYANAN

Department of Chemical Engineering, Sri Venkateswara College of Engineering, Tamil Nadu, India

ARTIFICIAL NEURAL NETWORK MODELING FOR DRYING KINETICS OF PADDY USING A CABINET TRAY DRYER

Article Highlights

- The drying temperature has a significant positive correlation on drying kinetics than air velocity
- ANN modeling with activation function TANSIGMOID shows the best prediction of drying kinetics
- ANN modeling shows exceptionally better prediction accuracy than mathematical modeling

Abstract

The study of drying kinetics and characteristics of agricultural products is essential for drying time estimation, designing dryers, and optimizing the drying process. Moisture diffusivity under different drying conditions is crucial to process and equipment design. The drying kinetics of paddy using a cabinet tray dryer was modeled using an Artificial Neural Network (ANN) technique. For predicting moisture ratio and drying rate, the Levenberg-Marquardt (LM) training algorithm with TANSIGMOID and TANSIGMOID hidden layer activation function provided superior results. A comparative evaluation of the predicting abilities of ANN and 12 different mathematical drying models was also carried out. The Midilli model was adequate for fitting the experimental data with an R^2 comparable to that of the ANN. However, the RMSE observed for ANN (0.0360) was significantly lower than that of the Midilli model (0.1673 to 0.712). Effective moisture diffusivity increased with an increase in temperature from 15.05 10^{-9} m^2/s to 28.5 10^{-9} m^2/s. The activation energy for drying paddy grains varied between 6.8 kJ/mol to 7.3 kJ/mol, which showed a moderate energy requirement for moisture diffusion.

Keywords: cabinet tray dryer, equilibrium moisture content, mathematical modeling, ANN modeling, effective diffusivity, activation energy.

SCIENTIFIC PAPER

UDC 66.047:66:632.51

Paddy (*Oryza Sativa* L.) is a staple food in most countries. It is regarded as one of the world's most essential nutritious staple food crops among cereals due to its use as human food and animal feed [1]. Drying is one of the earliest preservation procedures used to reduce the moisture content of biological materials to a level that inhibits microbial development and reduces the rate of deteriorative chemical reactions. Besides improving shelf life, drying allows for the development of a wide range of value-added goods from agricultural food [2]. The growing global demand for high-quality dried paddy rice has prompted the investigation of viable preservation solutions [3]. Cabinet tray drying is a versatile method because of its ease of operation. It is a ubiquitous drying technique. It retains the quality and nutritional content of dried material compared to sun drying, infrared drying, freeze-drying, fluidized bed drying, and dielectric drying [4]. The paddy will be spread out on the trays, with a heating medium (hot air) passing through. The drying process can be efficient by ensuring uniform airflow distribution across the trays. Besides many matematical

Correspondence: M. Narayanan, Department of Chemical Engineering, Sri Venkateswara College of Engineering, Pennalur, Sriperumbudur Tk, Kancheepuram Dt, Tamil Nadu - 602117, India.
E-mail: nmena@svce.ac.in
Paper received: 6 January, 2022
Paper revised: 6 May, 2022
Paper accepted: 21 July, 2022

https://doi.org/10.2298/CICEQ220106017S

models, artificial neural networks (ANNs) are a sophisticated computational tool for modeling complicated interactions between input and output parameters [5]. ANN analysis can produce more realistic and accurate forecasts [6]. Some of the notable pieces of literature are illustrated below (Table 1).

Table 1. Existing literature report.

Ref.	Year	Methodologies	Inferences
[5]	2016	Statistical analysis	— The drying temperature and tempering duration effects were investigated on drying kinetics and moisture diffusivity. The results showed that adding a tempering stage considerably impacted drying performance and effective moisture diffusivity. — Several thin layer drying models were fitted to experimental data of each drying stage, namely pre-tempering and post-tempering, and the models' appropriateness was assessed using statistical analysis. The Midilli and Tow-Term models were determined to be the most suitable for the first and second drying stages.
[6]	2016	ANN modeling	— Using six distinct models, thin-layer drying kinetic analysis of paddy dried under low-temperature conditions (20°C–40°C) and constant air velocity of 1.41 m/s was performed using a drying chamber. The Midilli model was found to be the best fit for describing the drying behavior of this species of paddy. — The drying constant for paddy drying increased with the drying temperature at low ambient temperatures (20°C–40°C).
[7]	2017	Third-order regression modeling	— The drying kinetics of high moisture paddy at 25% (wet basis) in a cylindrical drying bin were investigated about process variables such as inlet air temperature, rate of airflow, and bed depth. — The drying rate and moisture ratio increased with drying temperature and airflow rate.
[8]	2017	Mathematical and ANN modeling	— To estimate the drying curves of rough rice, a comparison was made between mathematical thin-layer models and artificial neural networks. — The kinetics of the thin layers of grains were investigated when the drying bed was separated into four thin layers (each 5 cm in height). According to the least *RMSE* and *chi-square* values, the Midilli model was the best for describing drying curves among the nine mathematical models employed for the prediction.
[9]	2018	Thermogravimetric analysis	— The thermogravimetric analyzer was used to investigate the isothermal drying kinetics of paddy with three initial dry basis moisture contents of 17.18, 21.05, and 30.12 percent. Under the drying temperature of 50 °C, the final moisture content of the three samples increased from 4.61 to 7.61 percent, with a rise in IMC from 17.18 to 30.12 percent. — The model proposed by Midilli is the most appropriate because the R^2 for the three samples was higher than the R^2 for the other four models.
[10]	2019	Regression analysis	— Paddy's drying kinetics and moisture diffusivity are investigated in a fluidized bed dryer. For drying paddy, different values of drying air temperatures (*T*) of 45 °C, 50 °C, and 55 °C, drying air velocities (*V*) of 2 m/s, 2.5 m/s, and 3 m/s, and paddy inventory of 2 kg and 3 kg are utilized. — The linear regression analysis obtains a regression equation correlating effective moisture diffusivity across all drying process parameters.
[11]	2020	ANN modeling	— To forecast M.R., the ANN approach was used. The impact of different drying processes on parboiled paddy's thermodynamic and qualitative parameters was investigated. Five mathematical approaches were used to predict the moisture ratio of parboiled rice. The results showed that as the intensity of the radiation, the temperature of the air, or the microwave power increased, the product surface temperature and moisture loss increased.
[12]	2021	Nonlinear regression analysis	— The drying kinetics model of paddy at a certain drying period was investigated in a swirling fluidized bed (SFB) drier. The drying was carried out at capacities of 1 kg, 2 kg, and 3 kg, with temperatures of 55 °C, a 45-minute drying duration, and an initial moisture content of 31.23 ± 0.26% percent (d.b.). A linear-plus-exponential model best describes the change in M.R. of paddy with time in the capacity range of 1 kg to 3 kg among the six drying kinetics models.
[13]	2021	ANN and adaptive neuro-fuzzy modeling	— The impact of hot air-drying kinetics on milled rice's quality and microstructural features during the instant controlled pressure drop (ICPD) assisted parboiling process was examined. In addition, the thin layer drying dynamics were studied using mathematical modeling. The Midilli model, which had the highest R^2 and the lowest *RMSE* and SSE values of the five mathematical models, predicted the best drying behavior of ICPD-treated parboiled rice grains.

However, considering the above inferences, the authors could not inspect any available literature investigating cabinet tray drying kinetics for paddy. Paddy drying kinetics prediction needs a more accurate and reliable method to attain better accuracy using evaluation metrics. Based on these needs, this work focused on the following objectives:

To assess the drying kinetics of paddy at different drying conditions; to estimate the equilibrium moisture content using the static gravimetric technique; to demonstrate ANN modeling using different activation functions such as TANSIGMOID, LOGSIGMOID, and PURELIN for paddy drying; To analyze the ANN modeling techniques using evaluation metrics such as

R^2, *RMSE*, and mean absolute error (*MAE*); To select and recommend the most accurate prediction technique to evaluate the drying kinetics of paddy.

MATERIAL AND METHODS

The paddy variety (rice CO 51) was collected from an agricultural field near Sriperumbudur, Tamilnadu, India. A paddy of fixed mass (100 g) was steeped in a constant temperature water bath for 3 hours at 45 °C, The excess water was drained, and surface moisture was removed by spreading it on the floor or using a muslin cloth. It has typically resulted in a moisture content of 26% on a dry basis. The conventional oven technique assessed the sample's initial moisture content (IMC). The convective cabinet tray dryer (Fig.1) was used for the study with only one tray in position, and it had a provision to control the temperature. The dimensions of the drying chamber were 250 mm x 250 mm x 300 mm with an air circulating fan (2HP centrifugal air blower). The air velocity was monitored and measured using a rotameter. A digital weighing balance with an accuracy of ±0.01 g was used to measure the weight loss. Paddy samples of approximately 100 g were dehydrated in a convective cabinet tray dryer at different drying temperatures of 40 °C, 50 °C, 60 °C, and 70 °C and air velocities of 1 m/s, 1.5 m/s, and 2 m/s. A thermostat was used to manage the tray dryer drying temperature. Moisture loss was measured every 5 minutes until equilibrium was established.

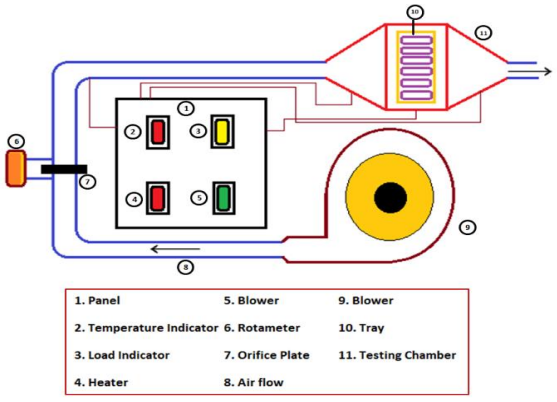

Figure 1. Schematic representation of cabinet tray dryer.

Radius of paddy

The volume displacement method using kerosene as the fluid was used to measure the paddy radius (*r*) by Eq. (1).

$$\text{Change in volume: } (V_f - V_i) = N \cdot \frac{4}{3}\pi r^3 \quad (1)$$

where N is number of dried paddy kernels, V_i is the initial volume of kerosene and V_f is the final volume of the kerosene.

$$\text{radius of the paddy: } r = \sqrt[3]{\frac{3\cdot(V_f - V_i)}{4\pi N}} \quad (2)$$

This method could only determine the approximate value of radius because the volume of individual paddy has been approximated to the volume of a perfect sphere. Therefore, the radius of the paddy grain is calculated to be 1.683 mm.

Equilibrium moisture content - relative humidity (EMC-RH)

The static gravimetric technique was utilized to determine the paddy's equilibrium moisture content (EMC) [14]. In a confined chamber, saturated solutions of different inorganic salts were used for sorption investigations to achieve regulated humidities ranging from 30% to 85% (5 levels), such as concentrated magnesium chloride, magnesium nitrate, sodium nitrate, sodium chloride, and potassium chloride. The sorption process was investigated at a temperature of 28 °C for paddy. For each of these trials, a 10 g sample of paddy was placed individually in desiccators in porous paper bags. The loss of moisture per unit weight of bone-dry material was used to calculate moisture content on a dry basis (d.b.). The increase or loss of weight of samples in each desiccator was tracked regularly until two successive measurements were consistent. Due to the nature of the samples, this took 36–40 days. For every sample, four homologs were preserved, and the average EMC values were taken. The moisture content of a paddy sample was tested by drying it for 24 hours at 105 °C. The samples were measured on a precision electronic balance with a least count of ±0.001 g. Eq. (3) is an appropriate model to estimate the EMC for paddy in the temperature range of 40 °C –70 °C and relative humidity (RH) of 30%–85% [15]:

$$-\ln(1-RH) = \beta(T)\cdot(M_e)^{\alpha} \quad (3)$$

where RH is the relative humidity, M_e is the equilibrium moisture content (d.b.) and T is the temperature (°C).

Determination of effective diffusivity

The effective diffusivity of spherical particles was evaluated using Eq. (4).

$$MR = \frac{6}{\pi^2}\sum_{n=1}^{\infty}\frac{1}{n^2}\exp\left(\frac{-n^2 D_{eff}\pi^2 t}{r^2}\right) \quad (4)$$

where D_{eff} is the effective diffusivity (m^2/s), r is the radius of the grain (m), t is the time of drying in seconds For long drying times, Eq. (4) can be further simplified to the first term of the series [16]. Thus Eq. (4) can be approximated in the logarithmic form to Eq. (5).

$$\ln MR = \ln \frac{6}{\pi^2} - \frac{\pi^2 D\ t}{r^2} \quad (5)$$

The most typical method for determining effective diffusivities is to plot experimental drying data in terms of *ln (MR)* vs. time. From Eq. (5), a plot of *ln(MR)* vs. *t* gives a straight line with a slope of $\pi^2 D / r^2$.

Effect of temperature on diffusivity

The temperature effect on diffusivity can be represented by the Arrhenius type of relationship (Eq.6).

The activation energy were calculated using relation is given by:

$$D = D_0 \exp\left(\frac{E_a}{RT}\right) \quad (6)$$

where D_0 is a constant, E_a is the activation energy required for moisture diffusion (kJ/mol), R is the Universal gas constant = 8.3144 J/mol K. D was measured at different temperatures to evaluate the constant D_0 and (E_a/R). Therefore, the above equation can be linearized as Eq.(7):

$$\ln D = \ln D_0 - E_a / RT \quad (7)$$

MODELING PROCESS

Mathematical modeling

The experimental moisture ratio (MR) data were fitted with twelve mathematical drying models (Table 1). First, the curve fitting tool in MATLAB version.2021 was used to determine the empirical constants and model performance metrics such as R^2, *RMSE*, and reduced chi-square (χ^2) in each model using regression analysis. Then, Eq. (1) was used to calculate the *MR* values.

$$MR = (M - M_e) / (M_0 - M_e) \quad (8)$$

where *MR* is the ratio of moisture, *M* is the moisture content at any time, M_0 is the initial moisture content, and M_e is the equilibrium moisture content. The best-fit coefficients of empirical models were evaluated by minimizing the mean square error between the measured data and predicted data by thin-layer drying models because it captured error between the actual and predicted data. The fmincon (minimum of inhibited nonlinear multivariable function) was used to curtail the *RMSE*. The highest R^2, the χ^2 and least *RMSE* were implied as error functions for the competence of the fit [17,18]. The statistical analysis parameters are represented as follows:

$$R^2 = 1 - \frac{\sum_{i=1}^{n}\left(MR_{\exp,i} - MR_{pre,i}\right)^2}{\sum_{i=1}^{n}\left(MR_{\exp,i} - MR'_{pre,i}\right)^2} \quad (9)$$

$$\chi^2 = \frac{\sum_{i=1}^{n}\left(MR_{\exp,i} - MR_{pre,i}\right)^2}{n - z} \quad (10)$$

$$RMSE = \frac{\sqrt{\left(MR_{\exp,i} - MR_{pre,i}\right)^2}}{n} \quad (11)$$

where $MR_{exp,i}$ is the i^{th} experimentally observed moisture ratio, $MR_{pre,i}$ is the i^{th} predicted moisture ratio, $MR'_{pre,i}$ is the mean average of predicted moisture ratio n is the number of observations, and z, the number of constants in models.

ANN modeling

ANNs have shown the upper hand in serving nonlinear programming over predictable modeling methods due to their rapid learning ability and suitability to nonlinear processes. An input layer, one or more hidden layer(s), and an output layer make up the ANN infrastructure. Each layer is made up of a collection of neurons or nodes. The internal connections between these nodes are known as weights, and they determine which nodes should be triggered based on the relative relevance of each signal. A mathematical activation function is used to process data in the nodes (e.g., TANSIGMOID, LOGSIGMOID, PURELIN, etc.) [19]. ANN learns from examples through iterations (epochs) without prior knowledge of the relationship between the variables being considered. ANN corrects the network by altering the internal connections based on the discrepancy between experimental and predicted results. This iterative process continues until the network predictions are reasonably accurate and consistent with the target data. Model simulations are used to obtain anticipated data once the training model has been tested and validated.

The data were modeled using a multiple-layer Feed-forward backpropagation algorithm network. One of the supervised learning techniques is the backpropagation algorithm (BP). The BP algorithm updates the weights by going ahead and backward until the output vector, and the predicted vector is as close as possible. Nonlinear mapping is a strong suit of the BP method. The primary benefit of adopting BP is that it can learn and adapt independently. Input data such as drying temperature, air velocity, and drying time make up the input layer. The output data, such as moisture ratio and drying rate, are stored in the output layer. 75% of the input data was utilized for training the network, with the remaining 25% being used to test the network. The Levenberg-Marquardt (LM) learning method was used to train ANN, a well-known efficient algorithm [19]. The adaptive learning algorithm was LEARNGDM (gradient descent with momentum weight and bias learning function). This ANN simulation was

done in MATLAB version.2021 with the ANN toolbox (command: NN tool). The number of neurons in the input hidden layer was varied to test various topologies. In addition, various permutations of activation functions in the hidden layers were employed. Standard statistical measures, including coefficient of determination (R^2), root mean square error (*RMSE*), and mean absolute error (*MAE*), were used to assess the predictability of the ANN model.

$$R^2 = 1 - \frac{\sum_{i=1}^{n}\left(y_{i,\exp} - y_{i,\mathrm{mod}}\right)^2}{\sum_{i=1}^{n}\left(y_{i,\exp} - y'_{i,\mathrm{mod}}\right)^2} \quad (12)$$

$$RMSE = \frac{\sqrt{\left(MR_{i,\exp} - MR_{i,\mathrm{mod}}\right)^2}}{n} \quad (13)$$

$$MAE = \frac{1}{n}\sum_{i=1}^{n}\left(y_{i,\exp} - y_{i,\mathrm{mod}}\right) \quad (14)$$

where n is the number of observations, $y_{i,exp}$ is experimental data, $y_{i,mod}$ is predicted data and $y'_{i,mod}$ is mean average of predicted data.

RESULTS AND DISCUSSION

Equilibrium moisture content - Relative humidity (EMC-RH)

The EMC and *RH* for the paddy were analysed. From the results, it was found that EMC decreases with temperature and increases with *RH*, as shown in Table 2. By fitting the data to Eq. (3). coefficients of the Henderson equation β and α were evaluated. β = 0.3461 and α = 2.164 [20]. The equilibrium moisture content at any other relative humidity and temperature can be easily measured by fitting the data to Henderson's equation (Eq. 3).

Table 2. EMC-RH data.

Relative humidity, %	Temperature, °C				
	28	40	50	60	70
	EMC				
33	7.92	7.51	7.40	7.30	7.20
52	9.94	9.90	9.98	9.96	9.53
64	11.56	11.54	11.42	11.26	11.10
75	13.14	13.10	13.05	12.90	12.79
84	16.13	15.18	14.96	14.75	14.55

Effect of drying temperature and air velocity

The moisture content was found to reduce with rising drying time. Moisture content was determined at various temperatures where the equilibrium was reached faster while increasing the temperature. However, removing the bound moisture at low temperatures requires extended time. In the case of higher temperatures (60 and 70) °C, the time taken to reach the equilibrium was less due to the higher diffusivity of moisture from the paddy to the surrounding air [21], the relative humidity of the drying air at a higher temperature was less compared to that at a lower temperature. Due to this reason, there was a higher rate of moisture diffusion as the temperature increased. Furthermore, it could be noted that the temperature affected the drying rate, and the total drying method was found to occur only in the falling rate period, as shown in Fig. 2. [22]. It specified that the method explaining the dehydration behavior of the paddy in a tray dryer was diffusion-governed [23].

Modeling of drying process by various mathematical models

The moisture ratio estimated from the experimental drying data at various temperatures and velocities was matched to twelve thin-layer models. The statistical parameters obtained from the regression analysis of these models are listed in Table 3. The R^2, *RMSE* and χ^2 values for the models varied between 0.899 to 0.999, 0.053 to 0.947, and 0.0001 to 0.0223, respectively. Hence, the model with the highest R^2 and the lowest χ^2 and *RMSE* was considered the best fit [24–27]. The Midilli model, in particular, was shown to be adequate in representing the tray drying behavior of paddy. The moisture ratio was calculated by considering the equilibrium moisture content, which is evaluated using Eq. (9). Fig. 3 was drawn between observed data and data predicted by the Midilli model at different temperatures and velocities [28]. Midilli model describes sufficiently well the drying characteristics of paddy at a given set of conditions [29,30].

Moisture ratio processing by ANN predictive modeling

Several topologies were tested by varying the number of processing elements (neurons) in the input hidden layer. The number of neurons in the hidden input layer varied to find the optimum number of processing elements. Several combinations of activation functions in the input hidden layer and output hidden layer were also employed. The number of processing elements and iterations (epoch) were recorded for each topology. Standard statistical parameters, like *RMSE*, *MAE*, and R^2 were employed to verify the accuracy of the prediction and validate the predictability of the ANN model [31]. After using various ANN topologies to the testing data, it was found that the network with TANSIGMOID – TANSIGMOID activation function combinations and five neurons in the input hidden layer gave the best result with maximum values of R^2, *RMSE*, and *MAE* of 0.9976, 0.0360, and 0.0034 were in accordance with the range reported in the

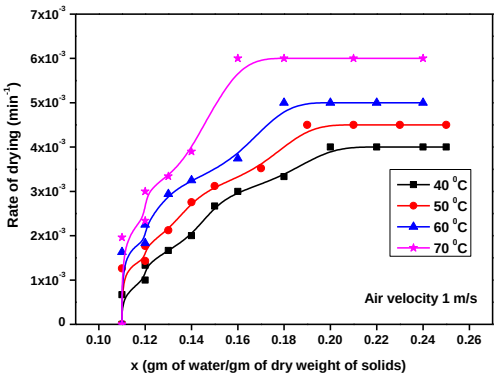

(a)

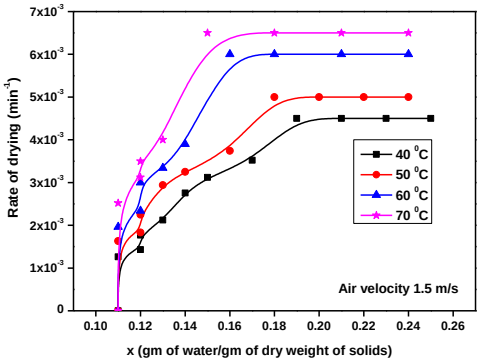

(b)

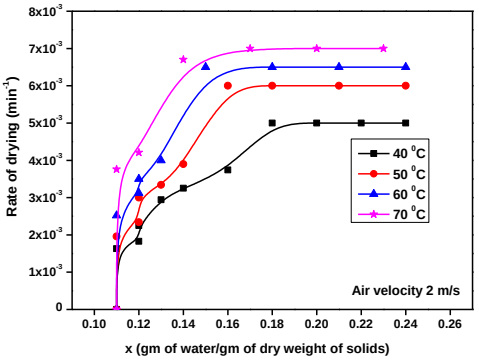

(c)

Figure 2. Rate of drying curves of paddy at different temperature and air velocity of (a) 1 m/s (b) 1.5 m/s (c) 2 m/s.

literature R^2 ranged from 0.981 to 0.999, *RMSE* ranged from 0.0333 to 0.1475 and *MAE* ranged from 0.05318 to 0.0088 [19,32].

Compared to other combinations, most training, validation, and testing data points for TANSIGMOID-TANSIGMOID activation function combinations and five neurons in the input hidden layer were closer to the equity line, indicating better fitness between experimental

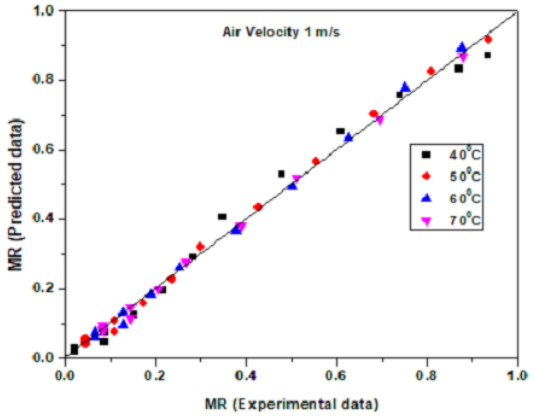

(a)

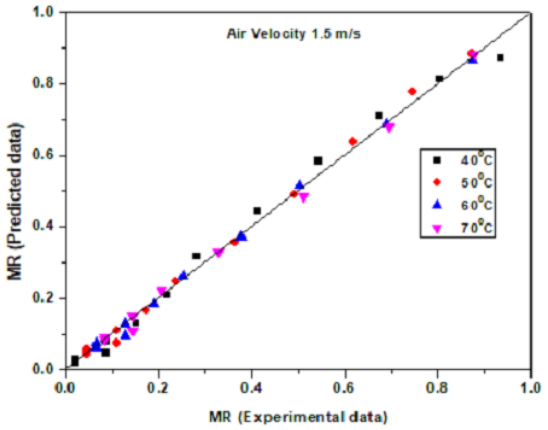

(b)

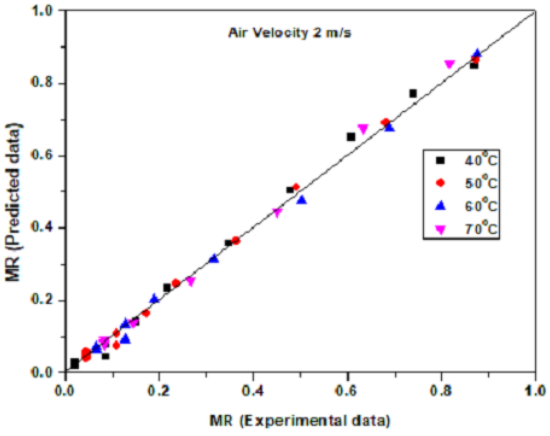

(c)

Figure 3. Experimental MR vs predicted MR by the Midilli model: (a) 1 m/s (b) 1.5 m/s (c) 2 m/s.

and ANN outputs shown in Fig.4. It was also noticed that TANSIGMOID - PURELIN activation function combinations, seven neurons in the input hidden layer showed the minimum deviation, and nine neurons in the input hidden layer with TANSIGMOID - LOGSIGMOID

Table 3. Results of statistical parameters estimated by regression analysis for paddy.

Model, MR =	Statistical parameters	Air velocity, m/s											
		1				1.5				2			
		Temperature °C											
		40	50	60	70	40	50	60	70	40	50	60	70
Page	R^2	0.998	0.997	0.995	0.992	0.999	0.996	0.993	0.981	0.997	0.995	0.982	0.987
$\exp(-kt^n)$	RMSE	0.845	0.573	0.513	0.457	0.834	0.596	0.499	0.571	0.840	0.578	0.612	0.636
	χ^2	0.0002	0.0005	0.0010	0.0019	0.0001	0.0007	0.0016	0.0046	0.00049	0.0011	0.0044	0.0033
Weibull distribution	R^2	0.991	0.994	0.998	0.996	0.992	0.997	0.992	0.992	0.991	0.998	0.993	0.993
$a-b\cdot\exp\left[-(kt^n)\right]$	RMSE	0.726	0.438	0.326	0.266	0.683	0.418	0.321	0.268	0.637	0.418	0.316	0.202
	χ^2	0.019	0.003	0.004	0.0001	0.0017	0.006	0.0012	0.0014	0.0018	0.0002	0.0001	0.0015
Henderson and Pabis	R^2	0.899	0.958	0.981	0.994	0.911	0.966	0.992	0.987	0.923	0.984	0.984	0.981
$a\cdot\exp(-kt)$	RMSE	0.947	0.754	0.545	0.449	0.752	0.702	0.484	0.566	0.570	0.586	0.595	0.626
	χ^2	0.0258	0.0101	0.0044	0.0013	0.0219	0.0078	0.0017	0.0030	0.0183	0.0034	0.0036	0.0047
Two term	R^2	0.964	0.952	0.976	0.992	0.911	0.966	0.987	0.983	0.923	0.984	0.978	0.969
$a\cdot\exp(-k_0t)+b\cdot\exp(-k_1t)$	RMSE	0.946	0.812	0.629	0.292	0.828	0.772	0.359	0.374	0.653	0.741	0.429	0.455
	χ^2	0.0216	0.017	0.0064	0.0017	0.0202	0.0076	0.0028	0.0039	0.0182	0.0042	0.0051	0.0073
Wang and Singh	R^2	0.984	0.991	0.996	0.997	0.989	0.995	0.997	0.994	0.995	0.997	0.993	0.993
$1+at+bt^2$	RMSE	0.732	0.442	0.332	0.318	0.624	0.397	0.363	0.401	0.567	0.437	0.458	0.302
	χ^2	0.0042	0.0021	0.0009	0.0005	0.0026	0.0010	0.0006	0.0014	0.0011	0.0006	0.0014	0.0017
Modified Page	R^2	0.998	0.997	0.995	0.992	0.999	0.996	0.993	0.981	0.997	0.995	0.982	0.987
$\exp\left[-(kt^n)\right]$	RMSE	0.845	0.573	0.513	0.457	0.834	0.596	0.499	0.571	0.840	0.578	0.612	0.636
	χ^2	0.0002	0.0005	0.0010	0.0019	0.0001	0.0007	0.0016	0.0046	0.0004	0.0011	0.0044	0.0033
Verma	R^2	0.913	0.958	0.979	0.991	0.926	0.969	0.988	0.983	0.940	0.982	0.979	0.978
$a\exp(-kt)+(1-a)\exp(-kt)$	RMSE	0.696	0.917	0.626	0.457	0.714	0.817	0.511	0.573	0.828	0.649	0.614	0.650
	χ^2	0.0274	0.0119	0.0055	0.0020	0.0223	0.0085	0.0027	0.0041	0.0171	0.0044	0.0053	0.0059
Lewis	R^2	0.926	0.948	0.972	0.986	0.913	0.944	0.981	0.972	0.934	0.962	0.981	0.983
$\exp(-kt)$	RMSE	0.759	0.958	0.791	0.676	0.657	0.904	0.715	0.757	0.546	0.806	0.784	0.806
	χ^2	0.0274	0.0119	0.0055	0.0020	0.022	0.0085	0.0027	0.0041	0.0171	0.0044	0.0053	0.0059
Simplifed Fick's diffusion	R^2	0.899	0.95	0.981	0.994	0.912	0.966	0.992	0.987	0.923	0.984	0.984	0.981
$a\exp\left(-c\left(t/L^2\right)\right)$	RMSE	0.947	0.754	0.545	0.449	0.752	0.702	0.484	0.566	0.570	0.586	0.595	0.626
	χ^2	0.0258	0.0101	0.0044	0.0013	0.0219	0.0078	0.0017	0.0030	0.0183	0.0034	0.0036	0.0047
Logarithmic	R^2	0.944	0.974	0.981	0.989	0.946	0.974	0.986	0.977	0.947	0.981	0.973	0.967
$a\exp(-kt)+c$	RMSE	0.686	0.708	0.545	0.379	0.562	0.690	0.451	0.460	0.454	0.582	0.523	0.582
	χ^2	0.0139	0.0063	0.0043	0.0025	0.0131	0.0060	0.0030	0.0054	0.0125	0.0042	0.0063	0.0081
Midilli	R^2	0.991	0.998	0.998	0.999	0.992	0.997	0.999	0.998	0.992	0.998	0.999	0.994
$a\exp\left(-kt^n\right)+bt$	RMSE	0.713	0.427	0.316	0.259	0.668	0.406	0.311	0.270	0.620	0.405	0.313	0.167
	χ^2	0.0020	0.0003	0.0004	0.0001	0.0017	0.0006	0.0001	0.0002	0.0018	0.0002	0.0002	0.0012
Two Term Exponential	R^2	0.913	0.958	0.979	0.991	0.926	0.969	0.988	0.983	0.997	0.995	0.982	0.987
$a\exp(-kt)+(1-a)\exp(-kat)$	RMSE	0.696	0.917	0.626	0.457	0.714	0.817	0.511	0.573	0.840	0.578	0.612	0.636
	χ^2	0.0274	0.0119	0.0055	0.0020	0.0223	0.0085	0.0027	0.0041	0.0004	0.0011	0.0044	0.0033

activation function combinations showed the least fit.

Using regression analysis and the Minitab version, a correlation was created between moisture ratio, drying time, drying temperature, and air velocity [33,34]. Fig.5 shows the schematic representation of ANN model topology.

$$MR = 0.000349t^2 - 0.000005T^2 - 0.0131v^2 + 0.000058Tt + 0.000286tv + 0.000083Tv - 0.04195t - 0.00531T - 0.081v + 1.523 \quad (15)$$

Drying rate processing by ANN predictive modeling

The number of neurons in the input hidden layer was changed to determine the optimal number of processing elements. Several activation functions were used in the input hidden layer and output hidden layer. The number of processing elements and iterations (epoch) for each topology was recorded. After applying different ANN topologies to the testing data, it was found that the network with TANSIGMOID-TANSIGMOID activation function combinations and

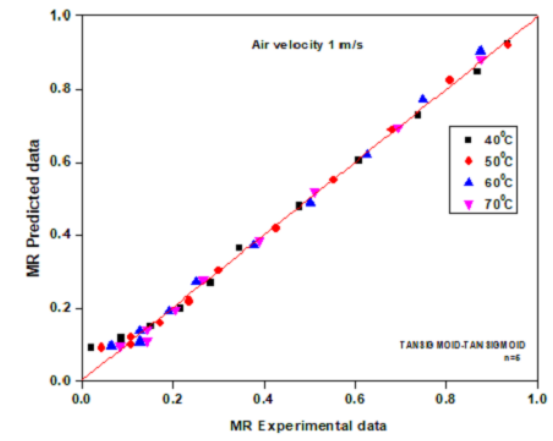

(a)

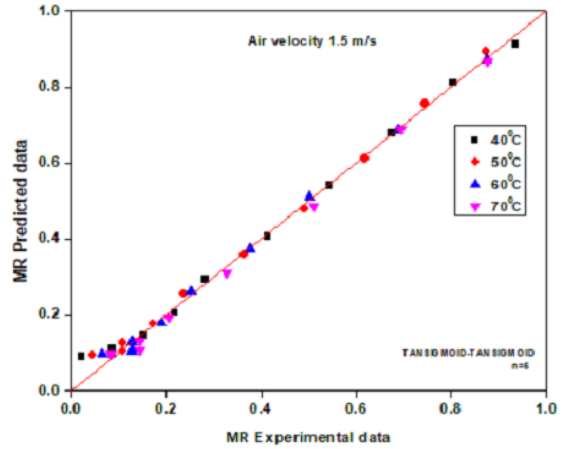

(b)

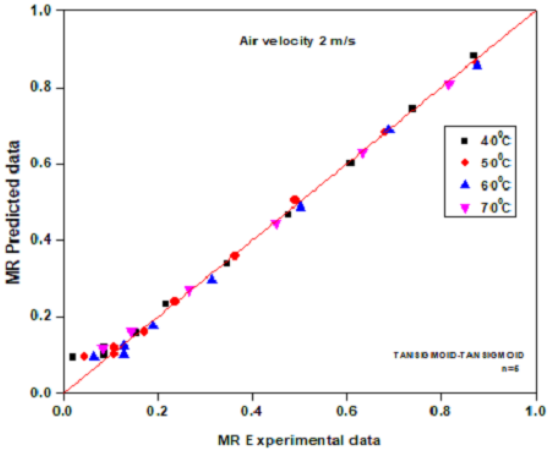

(c)

Figure 4. Comparison of experimental MR and predicted MR of ANN modeling using TANSIGMOID -TANSIGMOID activation function: (a) 1 m/s (b) 1.5 m/s (c) 2 m/s.

nine neurons in the input hidden layer produced the best results, with R^2, *RMSE*, and *MAE* values of 0.9696, 0.0916, and 0.0028 were in accordance with the range

reported in the literature, R^2 ranged from 0.981 to 0.999, *RMSE* ranged from 0.0333 to 0.1475, and *MAE* ranged from 0.05318 to 0.0088 [19,32].

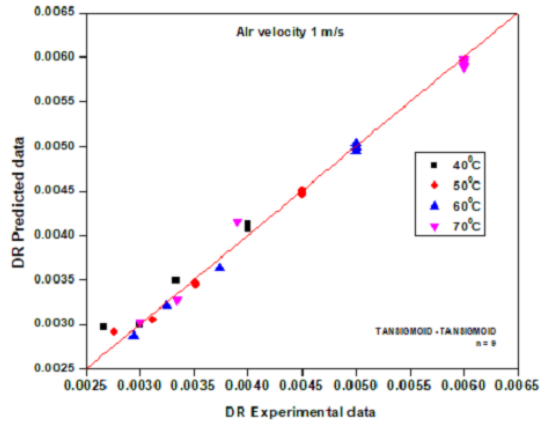

(a)

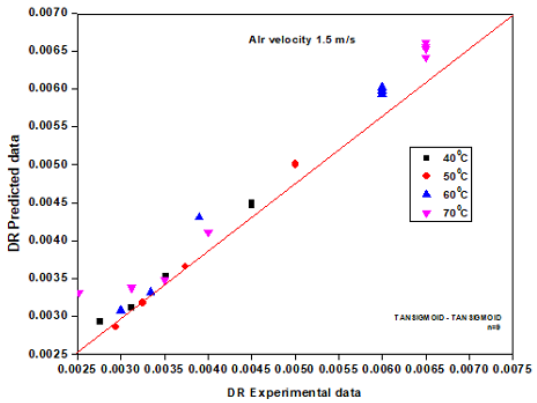

(b)

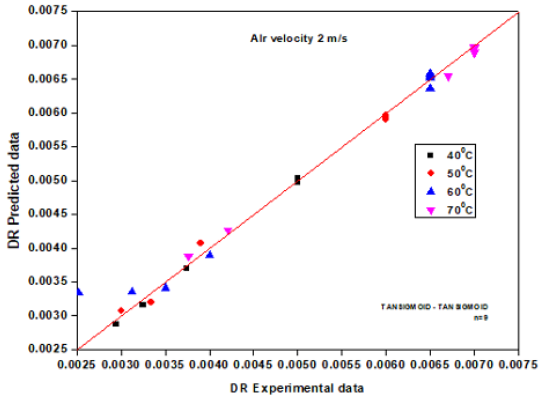

(c)

Figure 5. Comparison of experimental DR and predicted DR of ANN modeling using TANSIGMOID - TANSIGMOID activation function: (a) 1 m/s (b) 1.5 m/s (c) 2 m/s.

Similarly, the drying rate data predicted by the other models, most of the training, validation, and testing data points for TANSIGMOID-TANSIGMOID activation function combinations and nine neurons in

the input hidden layer were closer to the diagonal than for other combinations, indicating that the experimental and ANN outputs shown in Fig. 6 are the best fit. Eight neurons in the input hidden layer with TANSIGMOID - LOGSIGMOID activation function combinations have the least fit, whereas six neurons in the input hidden layer with TANSIGMOID - PURELIN activation function combinations have the reasonable fit. Using regression analysis, Minitab version.17 was used to build a correlation between drying rate, drying time, drying temperature, and air velocity.

$$DR = -0.000001t^2 - 0.000057v^2 - 0.000002tT - 0.000041tv - 0.000006Tv + 0.000126t + 0.000115T + 0.00214v - 0.00226 \quad (16)$$

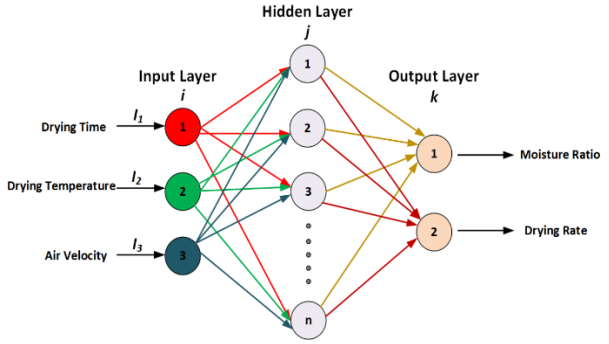

Figure 6. Schematic representation of ANN model.

ANN versus mathematical models

The twelve mathematical drying models had lower R^2 and higher *MSE* than the ANN (Table 4). The plot of experimental vs. predicted data (Fig. 4) and (Fig. 6) reveals that ANN accurately predicted the moisture ratio and drying rate for tray-dried paddy. Similarly, the independent of parameters used, the prediction capability of trained ANN was better than that of the investigated mathematical models, was reported by [35–38]. It is worth noting that the Midilli model was able to compete spiritedly with ANN's unique predictive capabilities, which were made possible by the lesser complexity of drying data. Fig. 7 shows a comparative analysis between different combinations of activation functions.

Determination of effective diffusivity

During the falling rate period, diffusion-controlled drying was investigated. It can be described by using Fick's diffusion equation [39,40]. Effective diffusivities of paddy for given temperatures and velocities were evaluated by Eq.(5). The effective diffusivity varied from 15.05 10^{-9} m^2/s to 28.5 10^{-9} m^2/s for paddy presented in Table 5. It was observed that the effective diffusivity was increased with the increased drying temperatures [41].

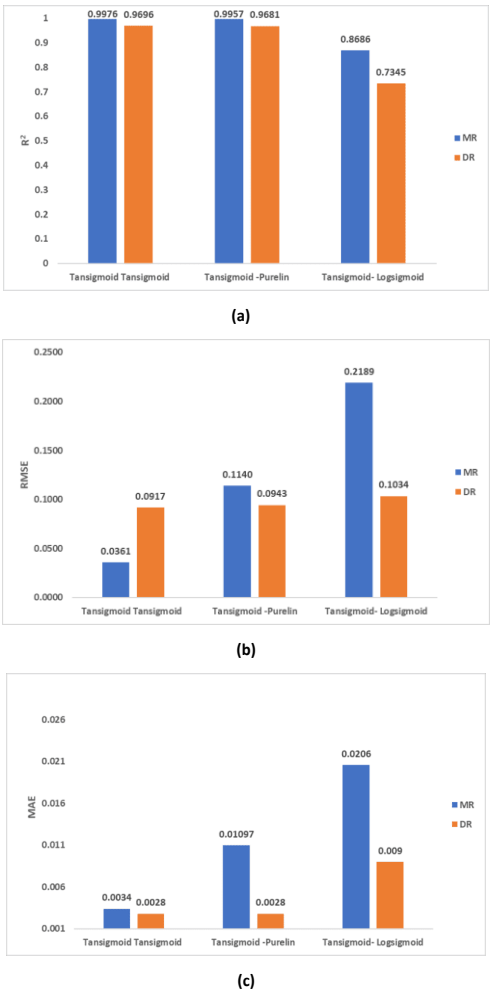

Figure 7. Comparative analysis between different combinations of activation functions: (a) R^2, (b) RMSE, (c) MAE.

Table 4. Comparative evaluation of ANN and selected semi-empirical model for a temperature range of (40–70) °C and air velocity range of (1–2) m/s.

Model	R^2	*MSE*
Midilli	0.991–0.999	0.028–0.508
ANN	0.9976	0.0013

However, no significant increment was observed due to increasing air velocities. Water evaporation occurred at the seed's surface, which was more immediately affected by temperature and velocity. Even with accelerated velocity and increasing temperature, the air had inadequate energy to release water molecules from the seed surface [42].

Effect of temperature on diffusivity

The activation energy was calculated from the slope of the Arrhenius plot, *ln(D)* versus *1/T*. The activation energy was evaluated to be 6.8 to 7.3 kJ/mol.

The majority of the water in paddy (like in other agricultural products) is bounded water. As a result, the drying process occurred at a falling rate. The drying and energy consumption rate increases with temperature and air velocity. If temperature increases, the water molecules gain more kinetic energy, leading to faster diffusion. The effect of temperature and air velocity on moisture diffusivity and activation energy in drying are shown in Table 6 [43].

Table 5. Effective diffusivity (m^2/s) at different temperatures and velocities.

Values	Air velocity, m/s											
	1				1.5				2			
	Temperature, °C											
	40	50	60	70	40	50	60	70	40	50	60	70
Slope	0.0524	0.0559	0.0614	0.0654	0.0711	0.0751	0.0795	0.0820	0.0782	0.0826	0.0868	0.0992
$D_{eff}10^{-9}$	15.05	16.06	17.62	18.81	20.43	21.58	22.86	23.56	22.47	23.72	24.93	28.50

Table 6. Data for diffusivity vs temperature.

	Air velocity, m/s											
	1				1.5				2			
1/T, 1/K	0.00319	0.00309	0.00300	0.00291	0.00319	0.00309	0.00300	0.00291	0.00319	0.00309	0.00300	0.00291
ln *D*	-18.01	-17.94	-17.85	-17.78	-17.70	-17.65	-17.59	-17.56	-17.61	-17.55	-17.50	-17.37
E_a, kJ	6.8				6.9				7.3			

CONCLUSION

Prediction of the drying kinetics of paddy was carried out using mathematical and ANN modeling. Specifically, twelve mathematical drying models and ANNs with different activation functions, such as TANSIGMOID, LOGSIGMOID, and PURELIN were evaluated. ANN models result in better prediction of drying kinetics. The accuracy level of the various activation functions was evaluated using model performance metrics. The following conclusions are made with the observed outcomes: ANN modeling attained exceptionally greater prediction accuracy than mathematical modeling based on the results of evaluation metrics. Among the three activation function, such as TANSIGMOID, LOGSIGMOID, and PURELIN, TANSIGMOID predicted the drying kinetics of paddy more precisely. R^2, *RMSE*, and *MAE*, performance metrics of ANN, showed a better scale of 0.9976, 0.0360, and 0.0034, respectively. Investigation of equilibrium moisture content revealed a direct relationship between relative humidity and drying temperature. It was observed that EMC and relative humidity increased as the temperature decreased.

REFERENCES

[1] M.R. Manikantan, P. Barnwal, R.K. Goyal, J. Food Sci. Technol. 51 (2014) 813–819. https://doi.org/10.1007/s13197-013-1250-1.

[2] S. Rajasekar, N. Meyyappan, D.G. Rao, ChemBioEng Rev. 4 (2017) 304–309. https://doi.org/10.1002/cben.201600018.

[3] O. Yaldýz, C. Ertekýn, Drying Technol. 19 (2001) 583–597. https://doi.org/10.1081/DRT-100103936.

[4] N. Norhadi, A.M. Akhir, N.R. Rosli, F. Mulana, Malaysian J. Chem.Eng. Technol. 3 (2020) 51–59. https://doi.org/10.24191/mjcet.v3i2.10965.

[5] R. Winiczenko, K. Górnicki, A. Kaleta, M. Janaszek-Mańkowska, Neural Comput. Appl. 30 (2018) 1795–1809. https://doi.org/10.1007/s00521-016-2801-y.

[6] V.K. Chasiotis, D.A. Tzempelikos, A.E. Filios, K.P. Moustris, Comput. Electron. Agric. 172 (2020). https://doi.org/10.1016/j.compag.2019.105074.

[7] M. Golmohammadi, M. Foroughi-dahr, M. R. Hamaneh, A. Reza, S. Jalaledin, Iran. J. Chem. Chem. Eng. 35 (2016) 105–117. https://doi.org/10.30492/IJCCE.2016.22064.

[8] S. Chakraborty, M. Sarma, J. Bora, S. Faisal, M.K. Hazarika, Agric. Eng. Int. 18 (2016) 177–189. https://cigrjournal.org/index.php/Ejounral/article/view/3645/2477.

[9] A.D. Arjun, S. Ganapathy, T. Pandiarajan, K. Bhuvaneswari, M. Duraisamy, Int. J. Agric. Eng. 10 (2017) 623–630. https://doi.org/10.15740/HAS/IJAE/10.2/623-630.

[10] M. Beigi, M. Torki-Harchegani, M. Mahmoodi-Eshkaftaki, Chem. Ind. Chem. Eng. Q. 23 (2017) 251–258. https://doi.org/10.2298/CICEQ160524039B.

[11] J. Zhang, P. Ma, X. Zhang, B. Wang, J. Wu, X. Xing, J. Therm. Anal. Calorim. 134 (2018) 2359–2365. https://doi.org/10.1007/s10973-018-7716-7.

[12] B. Pattanayak, S.S. Mohapatra, H.C. Das, Int. J. Postharvest Technol. Innov 6 (2019) 162–178. https://doi.org/10.1504/IJPTI.2019.106194.

[13] E. Taghinezhad, A. Szumny, M. Kaveh, V.R. Sharabiani, A. Kumar, N. Shimizu, Foods 9 (2020) 1–17.

https://doi.org/10.3390/foods9010086.

[14] A. Sitorus, Novrinaldi, S.A. Putra, I.S. Cebro, R. Bulan, Case Stud. Therm. Eng. 28 (2021) 1–9. https://doi.org/10.1016/j.csite.2021.101572.

[15] S. Chakraborty, S.P. Gautam, M. Sarma, M.K. Hazarika, Food Sci. Technol. Int. 27 (2021) 746–763. https://doi.org/10.1177/1082013220983953.

[16] M. Lutovska, V. Mitrevski, I. Pavkov, M. Babic, V. Mijakovski, T. Geramitcioski, Z. Stamenkovic, J. Process. Energy Agric. 21 (2017) 91–96. https://scindeks.ceon.rs/article.aspx?artid=1821-44871702091L.

[17] D.G. Rao, B.S. Sridhar, G. Nanjundaiah, J. Food Eng. 17 (1992) 49–58. https://doi.org/10.1016/0260-8774(92)90064-D.

[18] M. Ahmet Tütüncü, T.P. Labuza, J. Food Eng. 30 (1996) 433–447. https://doi.org/10.1016/S0260-8774(96)00028-3.

[19] T. Gunhan, V. Demir, E. Hancioglu, A. Hepbasli, Energy Convers. Manage. 46 (2005) 1667–1679. https://doi.org/doi:10.1016/j.enconman.2004.10.001.

[20] R.L. Sawhney, P.N. Sarsavadia, D.R. Pangavhane, S.P. Singh, Drying Technol. 17 (1999) 299–315. https://doi.org/10.1080/07373939908917531.

[21] A. Tarafdar, N. Jothi, B.P. Kaur, J. Appl. Res. Med. Aromat. Plants 24 (2021) 1–8. https://doi.org/10.1016/j.jarmap.2021.100306.

[22] G.O. Ondier, T.J. Siebenmorgen, R.C. Bautista, A. Mauromoustakos, Trans. ASABE. 50 (2011) 1007–1013. https://doi.org/10.13031/2013.37085.

[23] J.O. Ojediran, A.O. Raji, Int. Food Res. J. 17 (2010) 1095–1106. http://www.ifrj.upm.edu.my/17%20(04)%202010/(30)%20IFRJ-2010-042%20Raji%20Nigeria[1].pdf.

[24] V.C. Siqueira, R.A. Leite, G.A. Mabasso, E.A.S. Martins, W.D. Quequeto, E.P. Isquierdo, Cienc. Agrotecnol. 44 (2020) 1–10. https://doi.org/10.1590/1413-7054202044011320.

[25] S. Rafiee, A. Keyhani, A. Jafari, Int. J. Food Prop. 11 (2008) 223–232. https://doi.org/10.1080/10942910701291858.

[26] B.H. Hassan, A.I. Hobani, J. Food Process Eng. 23 (2000) 177–189. https://doi.org/10.1111/j.1745-4530.2000.tb00510.x.

[27] I.L. Pardeshi, S. Arora, P.A. Borker, Drying Technol. 27 (2009) 288–295. https://doi.org/10.1080/07373930802606451.

[28] N.A. Akgun, I. Doymaz, J. Food Eng. 68 (2005) 455–461. https://doi.org/10.1016/j.jfoodeng.2004.06.023.

[29] Xiao-Kang Yi, Wen-Fu Wu, Ya-Qiu Zhang, Jun-Xing Li, Hua-Ping Luo, Math. Probl. Eng. (2012) 1–19. https://doi.org/10.1155/2012/386214.

[30] Y.G. Keneni, A.K. (Trine) Hvoslef-Eide, J.M. Marchetti , Ind. Crops Prod. 132 (2019) 12–20. https://doi.org/10.1016/j.indcrop.2019.02.012.

[31] Qing-An Zhang, Yun Song, Xi Wang, Wu-Qi Zhao, Xue-Hui Fan, CYTA J. Food 14 (2016) 509–517. https://doi.org/10.1080/19476337.2015.1136843.

[32] S. Soodmand-Moghaddam, M. Sharifi, H. Zareiforoush, H. Mobli, Qual. Assur. Saf. Crop.12 (2020) 57–66. https://doi.org/10.15586/QAS2019.658.

[33] P. Thant, P. Robi, P. Mahanta, Int. J. Eng. Appl. Sci. 5 (2018) 118–123. https://www.ijeas.org/download_data/IJEAS0503034.pdf.

[34] A. Sitorus, Novrinaldi, S.A. Putra, I.S. Cebro, R. Bulan, Case Stud. Therm. Eng. 28 (2021). https://doi.org/10.1016/j.csite.2021.101572.

[35] S. Kono, I. Kawamura, T. Araki, Y. Sagara, Int. J. Refrig. 65 (2016) 218–227. https://doi.org/10.1016/j.ijrefrig.2015.10.009.

[36] B. Osodo, D. Nyaanga, J. Kiplagat, J. Muguthu, Am. J. Food Technol. 6 (2018) 263–271. http://pubs.sciepub.com/ajfst/6/6/6/.

[37] M. Kashiri, A.D. Garmakhany, A.A. Dehghani, Qual. Assur. Saf. Crop. Foods 4 (2012) 179–184. https://doi.org/10.1111/j.1757-837X.2012.00184.x.

[38] I. Golpour, R. Amiri Chayjan, J. Amiri Parian, J. Khazaei, J. Agric. Sci. Technol. 17 (2015) 287–298. https://jast.modares.ac.ir/article-23-10165-en.pdf.

[39] U. Şahin, H.K. Öztürk, J. Food Process Eng. 41 (2018) 1–14. https://doi.org/10.1111/jfpe.12804.

[40] J.W. Bai, H.W. Xiao, H. L. Ma, C.S. Zhou, J. Food Qual. (2018) 1–9. https://doi.org/10.1155/2018/3278595.

[41] M. Garg, S. Sharma, S. Varmani, S. Sadhu, Int. J. Food Sci. Nutr. 3 (2014) 61–66. https://www.researchgate.net/publication/341440997_DRYING_KINETICS_OF_THIN_LAYER_PEA_PODS_USING_TRAY_DRYING#fullTextFileContent.

[42] A. Motevali, S. Younji, R.A. Chayjan, N. Aghilinategh, A. Banakar, Int. Agrophys. 27 (2013) 39–47. https://doi.org/10.2478/v10247-012-0066-y.

[43] A. Fernandez, C. Román, G. Mazza, R. Rodriguez, Case Stud. Therm. Eng. 12(2018) 248–257. https://doi.org/10.1016/j.csite.2018.04.015.

RAJASEKAR SUBRAMANYAM
MEYYAPPAN NARAYANAN

Department of Chemical Engineering, Sri Venkateswara College of Engineering, Tamil Nadu, India

NAUČNI RAD

MODELOVANJE KINETIKE SUŠENJE PIRINČA U SUŠARI SA TAVAMA VEŠTAČKOM NEURONSKOM MREŽOM

Proučavanje kinetike sušenja i karakteristika poljoprivrednih proizvoda je od suštinskog značaja za procenu vremena sušenja, projektovanje sušara i optimizaciju procesa sušenja. Difuzivnost vlage u različitim uslovima sušenja je ključna za projektovanje procesa i opreme. Kinetika sušenja pirinča u sušari sa tavama je modelovana korišćenjem veštačke neuronske mreže (ANN). Levenberg-Markuardt (LM) algoritam za obuku sa funkcijama aktivacije skrivenog sloja TANSIGMOID i TANSIGMOID dao je superiorne rezultate u predviđanju odnosa vlage i brzine sušenja. Takođe, izvršena je komparativna procena prediktivnih sposobnosti ANN i 12 različitih matematičkih modela sušenja. Midilijev (Midillijev) model adekvatno opisuje eksperimentalne podatke sa vrednošću koeficijenta determinacije R^2 koja uporediva sa vrednošću za ANN. Međutim, RMSE za ANN (0,0360) je značajno niži od onog kod Midilijevog modela (0,167 do 0,712). Efektivna difuzivnost vlage se povećava sa porastom temperature sa 15,05 x 10^{-9} m^2/s na 28,5 x 10^{-9} m^2/s. Energija aktivacije za sušenje zrna pirinča varirala je između 6,8 kJ/mol i 7,3 kJ/mol, što je pokazalo umerenu potrebu za energijom za difuziju vlage.

Ključne reči: sušara sa tavama, ravnotežni sadržaj vlage, matematičko modelovanje, ANN modelovanje, efektivna difuzivnost, energija aktivacije.